Selection mechanism for rotating patterns in weakly excitable media

Vladimir S. Zykov
Institut für Theoretische Physik, Technische Universität Berlin, D-10623 Berlin, Germany
(Received 5 September 2006; revised manuscript received 2 February 2007; published 5 April 2007)

Two types of patterns rigidly rotating within a disk of a weakly excitable medium are studied using the free-boundary approach. The patterns are spots moving along the boundary of the disk and spiral waves rotating around the disk center. The study reveals a selection mechanism that uniquely determines the shape and the angular velocity of these patterns as a function of the medium excitability and the disk radius. These two types of patterns coexist below some critical parameter value, coincide at a bifurcation point, and do not exist above it. The same selection mechanism is applied to describe a limiting case of a spiral wave rotating in an unbounded medium.

DOI: 10.1103/PhysRevE.75.046203 PACS number(s): 82.40.Bj, 05.45.−a, 05.65.+b, 47.54.−r

I. INTRODUCTION

Wave patterns propagating in excitable media play a very important role in diverse physical, chemical, or biological processes. Self-organized formation of wave patterns in excitable media represents a broad and intensively developed field of study in nonlinear dynamical systems and has potential applications, e.g., in cardiology [1–4].

Rigidly rotating spirals, critical fingers, and wave segments are common moving patterns in weakly excitable two-dimensional media. Most famous are spiral waves, often used as a paradigmatic example of the self-organization [3]. Wave segments are inherently unstable, but they can be easily stabilized by applying an appropriate feedback to the excitability of the medium [5]. They define a separatrix between spiral wave behavior and contracting wave segments [6]. Unbounded wave segments (critical fingers) lie on the asymptote of this separatrix, defining the boundary between excitable and subexcitable media [7,8].

The pattern selection problem has been successfully solved for critical fingers [7,9] and for wave segments [6]. The situation with a selection mechanism for spiral waves is more complicated. The theory describing spiral waves in highly excitable media is well-developed under the assumption that the spiral wave core is small [10]. However, it fails to consider the limit of a weak excitability when both the rotation period and the core size of a spiral wave diverge. The kinematical theory developed in [4], especially for the case of a large core size, assumes boundary conditions, which cannot be derived rigorously. The asymptotic analysis, aimed to describe a spiral wave in a weakly excitable medium as a slightly deformed critical finger [9], is oriented on the consideration of unbounded media and cannot be applied to study the role of the medium size, i.e., to describe spiral waves rotating within a disk.

Thus although spiral waves rotating within a disk have been obtained in numerical computations and observed in experiments [11–16], the corresponding theory is still ill-elaborated in the limit of weakly excitable media.

In this paper a unified approach is proposed which allows us first to formulate a pattern selection principle for an excitation spot rotating along the boundary of a disk. Then this problem is generalized to consider a spiral wave rotating around the disk center. It is shown that these two solutions coexist and coincide at a critical value of the excitability. The selection mechanism for spiral waves rigidly rotating in an unbounded medium follows from this unified description as a limiting case of a disk of an infinitely large size. Because no assumption about the size of the spiral wave core is used, this approach is applicable to the case of a weakly excitable medium, up to the critical finger limit.

II. EXCITABLE MEDIA MODEL

Our aim is to reveal a universal selection mechanism for wave patterns rotating in excitable media with different kinetics. The following two-variable reaction-diffusion model is used as an example of such a medium:

$$\frac{\partial u}{\partial t} = D\nabla^2 u + F(u,v),$$

$$\frac{\partial v}{\partial t} = \epsilon G(u,v), \tag{1}$$

where the variables $u(x,y,t)$ and $v(x,y,t)$ represent, respectively, the activator and the inhibitor in a two-dimensional medium. Typically $\epsilon \ll 1$, and the activator u is treated as a fast variable with respect to the slow inhibitor v.

For the functions $F(u,v)$ and $G(u,v)$, we take the FitzHugh-Nagumo type form used previously [7]:

$$F(u,v) = 3u - u^3 - v,$$

$$G(u,v) = u - \delta, \tag{2}$$

with $\delta = -1.6797$.

This system has a single uniform resting state $(u_0, v_0) = (\delta, 3\delta - \delta^3)$. Here u_0 is the smallest root of the cubic equation $F(u,v_0)=0$. For the given value of δ, $|v_0| = 0.3$, that is small compared with $|u_0| \approx \sqrt{3}$.

The resting state is stable with respect to small perturbations. However, a suprathreshold perturbation applied uniformly to the whole medium induces a transition to the excited state (u_e, v_0), where u_e is the largest root of the equation $F(u,v_0)=0$. During the excited state the inhibitor v slowly

 ©2007 The American Physical Society

changes, due to Eq. (1). After a finite time interval inversely proportional to ϵ, this change is followed by a jump of the activator value to the left branch of the nullcline $F(u,v)=0$ [1,4,7,12]. Then the medium slowly returns back to the resting state.

A suprathreshold local perturbation or specific initial conditions induce a propagating excitation wave with a sharp jump of the activator value between the resting and excited states. During this jump the value of the slow inhibitor v remains practically constant, while the activator u makes a rapid change between $u_0 \approx -\sqrt{3}$ and $u_e \approx \sqrt{3}$. This part of the propagating wave represents a wave front. The excited state is followed by a rapid change of the activator in the opposite direction, from u_e to u_0. This is the back of the excitation wave.

III. ROTATING PATTERNS WITHIN A DISK WITH NO-FLUX BOUNDARY

Free boundary formulation has been used by many authors to study pattern selection in two-dimensional excitable media [9,10,12,17–20]. This approach reduces the problem of wave propagation in a reaction-diffusion system to the kinematics of a sharp interface separating regions of the excited and resting states of the medium.

The propagation velocity c_p of a planar interface is a monotonically decreasing function of the slow variable v at the moving boundary layer, vanishing at a value $v=v^*$. If v is close to v^*, the wave velocity is approximated by a linear function [12]:

$$c_p(v) = \alpha\sqrt{D}(v^* - v). \tag{3}$$

The coefficients α and v^* are uniquely determined by $F(u,v)$. For instance, for the cubic function defined by Eq. (2), $\alpha=\sqrt{1/2}$ and $v^*=0$ [7].

Obviously, the value of v at the very first excitation front generated in the medium is equal to the value v_0 corresponding to the resting state. Since the rotation period of a pattern rotating in a weakly excitable medium is large, it is assumed that the medium has enough time to completely recover to the resting state during the time interval between two pulses. Thus one can neglect the refractory properties of the medium, if the rotation period of a pattern is large enough [1,4,7,12]. Then, in accordance with Eq. (3), the propagation velocity of the wave front even for a periodically rotating pattern is determined by the quantity $\Delta=v^*-v_0$ and can be written as

$$c_0 = \alpha\Delta\sqrt{D}. \tag{4}$$

Figure 1(a) shows an example of a rotating wave pattern in a two-dimensional medium. This is an excitation spot moving along the no-flux boundary of a disk. The moving interface includes segments, where $du/dt>0$ (wave front) and $du/dt<0$ (wave back). The inner ends of the front and the back coincide at the so-called phase change point, where $du/dt=0$ [21], while the other ends are pinned to the no-flux boundary of the disk. It is convenient to parametrize the shape and the velocity of the spot boundary by the arclength

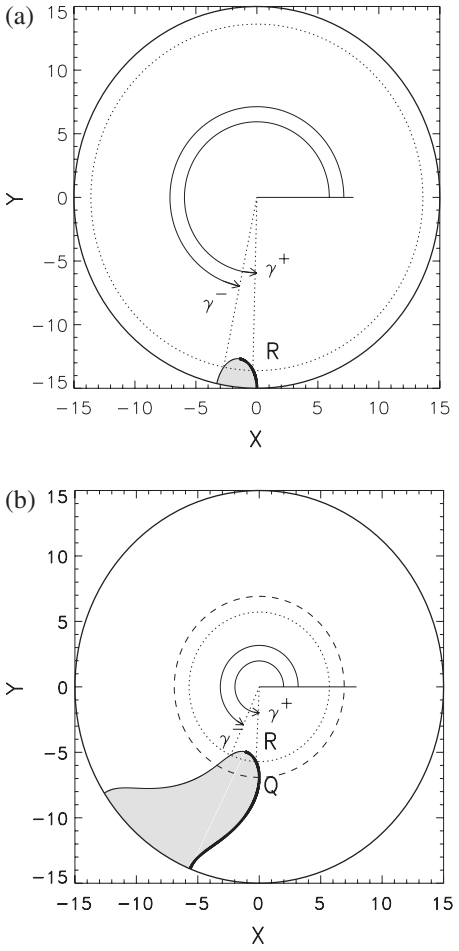

FIG. 1. Two types of wave patterns rotating in a disk of radius $R_D=15$. (a) Excitation spot moving along the disk boundary with the angular velocity $\Omega=0.049$. (b) Spiral wave rotating around the disk center at $\Omega=0.1$. The front (thick solid) and the back (thin solid) of both patterns obey Eqs. (11)–(14) with $B=0.3247$.

s, counted from the phase change point, assuming that $s<0$ for the points of the back. Let us denote by $c_n(s)$ the normal velocity, by $c_\tau(s)$ the tangential velocity, and by $k=k(s)$ the local curvature of the boundary. It was shown [4] that these three functions obey the following system of differential equations:

$$\frac{dc_n}{ds} = \omega + kc_\tau, \tag{5}$$

$$\frac{dc_\tau}{ds} = -kc_n, \tag{6}$$

where ω is the angular velocity of a rigidly rotating pattern. It is also known that the normal velocity c_n depends on the local curvature k [4,12]

$$c_n = c_p(v) - Dk. \tag{7}$$

In accordance with Eq. (1), within the excited region the slow variable v varies along a circle of radius r as

$$\omega dv/d\gamma = -\epsilon G(u_e(v),v), \tag{8}$$

where γ is the polar angle.

For $\Delta \ll 1$, the value $G(u_e(v),v)$ in this equation remains practically constant, $G^*=G(u_e(v^*),v^*)$, and the value of the slow variable at the wave back reads as

$$v^-(r) = v_0 + \frac{G^*\epsilon}{\omega}[\gamma^+(r) - \gamma^-(r)], \tag{9}$$

where γ^+ (γ^-) specifies the location of the front (back) of the spot. The substitution of this expression into Eqs. (3) and (7) yields the velocity of the back

$$c_n^-(r) = c_0 - \frac{G^*\epsilon\alpha\sqrt{D}}{\omega}[\gamma^+(r) - \gamma^-(r)] - Dk^-(r). \tag{10}$$

After rescaling ($S=sc_0/D$, $R=rc_0/D$, $C=c/c_0$, $K=Dk/c_0$, and $\Omega=\omega D/c_0^2$) Eqs. (5)–(7) and (10), transform into the dimensionless form

$$\frac{dC_n}{dS} = \Omega + KC_\tau, \tag{11}$$

$$\frac{dC_\tau}{dS} = -KC_n, \tag{12}$$

$$C_n^+ = 1 - K^+, \tag{13}$$

$$C_n^-(R) = 1 - \frac{B}{\Omega}[\gamma^+(R) - \gamma^-(R)] - K^-(R), \tag{14}$$

where

$$B = \frac{G^*\epsilon}{\alpha^2\Delta^3}. \tag{15}$$

The dimensionless parameter B characterizes the excitability of the medium, like it does in the case of a critical finger [7] or a wave segment [6]. In particular, an undamped propagation of an excitation wave in a two-dimensional medium is possible only if $B<B_c\approx 0.535$ [7]. In a weakly excitable medium the parameter B should be close to B_c. Our aim now is to demonstrate that this parameter uniquely determines the angular velocity and the shape of a rotating spot.

Let K_{DR} be the curvature of the front and S_{DR}^+ be the arclength of the front at the disk boundary. Then the normal velocity of the front at the boundary is determined by Eq. (13) as $C_n^+(S_{DR}^+)=1-K_{DR}$. Since the front is orthogonal to the no-flux boundary of the disk, the angular velocity Ω is given by the simple expression

$$\Omega = (1 - K_{DR})/R_D, \tag{16}$$

where R_D is the disk radius. In addition, the tangential velocity of the front has to be zero at the disk boundary due to the orthogonality. Thus in order to determine the front shape we need to integrate the system (11)–(13) with Ω specified by Eq. (16) and with the following initial conditions:

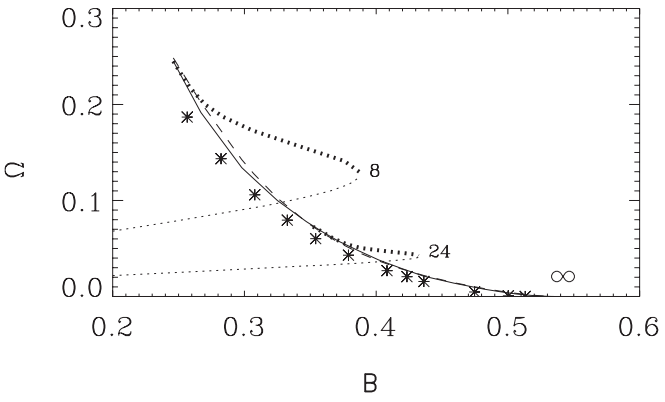

FIG. 2. Angular velocity of a spot (thin dotted lines) and of a spiral wave (thick dotted lines) obtained as a solution of the free-boundary problem for two different disk radii $R_D=8$ and 24. The thin solid line shows angular velocity of an unbounded spiral. The prediction following from Eqs. (25) and (26) is shown by a dashed line. Separate stars show results of direct integrations of the models (1) and (2).

$$K^+(S_{DR}^+) = K_{DR}, \quad C_\tau(S_{DR}^+) = 0. \tag{17}$$

Integration of the system (11)–(13) in the reverse arclength direction uniquely determines the shape of the front for given $K_{DR}>0$. This integration has to be carried out until the phase change point, where C_n^+ vanishes. This procedure determines the Cartesian and polar coordinates of the front and the tangential velocity of the phase change point $C_\tau(0)=C_t$.

These data are necessary to integrate Eqs. (11), (12), and (14) for the spot back with Ω determined by Eq. (16). The initial conditions for this integration are

$$K^-(0) = 1, \quad C_\tau(0) = C_t. \tag{18}$$

These initial conditions completely determine the solution, which will, however, depend on the parameter B. Using a trial and error method one must vary the value of B until the corresponding solution satisfies another boundary condition

$$C_\tau(S_{DR}^-) = 0. \tag{19}$$

Repetition of these computations for different K_{DR} and R_D yields the dependence $B=B_{PS}(R_D,K_{DR})$. Note that since the angular velocity Ω is also a function of R_D and K_{DR}, due to Eq. (16), these computations specify the dependence $\Omega=\Omega_{PS}(B,R_D)$. Figure 2 shows this dependence computed for two disk radii $R_D=8$ and 24.

Rotating wave patterns in a form of a spot moving along the no-flux boundary of a disk have been unknown before this study. They are intrinsically unstable and can be observed in excitable media only under a stabilizing feedback, similarly to the wave segments [6]. Obviously, the rotating spots are transforming into the wave segments in the limit $R_D\to\infty$. The free-boundary approach creates the opportunity to determine the shape of a spot, as illustrated by Fig. 1(a), and its angular velocity, which is an increasing function of the parameter B, as shown in Fig. 2.

Another type of pattern rotating within a disk is a spiral wave, as illustrated in Fig. 1(b). This pattern is computed for a disk of the same size, as in Fig. 1(a), and the excitability of the medium is the same. The wave is rotating at a higher angular velocity than the spot velocity and the arclength of the front is considerably larger. Moreover, there are two points at the front, where the tangential velocity C_τ vanishes. One point is located at the disk boundary, like in the case of a spot. However, the front curvature at this point is negative $K^+(S^+_{DR})<0$ in contrast to the spot front shown in Fig. 1(a). Due to this, there is some inner point of the front, point Q, where the tangential velocity vanishes. Here the normal velocity is orthogonal to the radial direction, and this point describes a closed pathway centered at the disk center [4,13].

Let K_Q be the front curvature at the point Q. To determine the shape of the outer part of the front, from point Q until the disk boundary, the system (11)–(13), has to be integrated assuming that at the point Q

$$K^+(S_Q) = K_Q, \quad C_\tau(S_Q) = 0. \tag{20}$$

The solution obtained will depend on the value of the angular velocity Ω. Using a trial and error method one must vary the value of Ω until the corresponding solution satisfies another condition at the disk boundary:

$$C_\tau(S^+_{DR}) = 0. \tag{21}$$

The next step is to find out the inner part of the front. To this aim, in analogy to a rotating spot, we start the integration of the system (11)–(13) with the boundary conditions

$$K^+(S_Q) = K_Q, \quad C_\tau(S_Q) = 0, \tag{22}$$

taking into account that Ω was already determined during the previous step. The integration has to be carried out in the reverse arclength direction until the phase change point, where $C^+_n=0$. As a result, the shape of the front and the tangential velocity of the phase change point C_t are determined by the given R_D and $0<K_Q<1$.

The data obtained have to be used to integrate the system (11), (12), and (14) for the spiral wave back with Ω determined for the outer part of the front. The initial conditions for this integration are given by Eq. (18). They completely determine the solution, which will depend only on the parameter B. Using a trial and error method one must vary the value of B until the corresponding solution satisfies another boundary condition (19). Repetition of this process for different K_Q and R_D yields the dependence $B=B_{RS}(R_D,K_Q)$. Since the angular velocity Ω is also a function of these two arguments, the proposed method allows us to specify the dependence $\Omega=\Omega_{RS}(B,R_D)$. Figure 2 shows this dependence computed for two different disk radii.

It is clearly seen in Fig. 2 that the angular velocity Ω of a spiral is a monotonically decreasing function of the parameter B, in contrast to the increasing angular velocity of a spot. These two solutions coexist below some critical value of B, as illustrated in Fig. 1, coincide at this critical point, and do not exist above this critical value. As it was mentioned above, the curvature of the spot front near the disk boundary is positive, while the curvature of the spiral front is negative here. At the critical value of B both curvatures vanish.

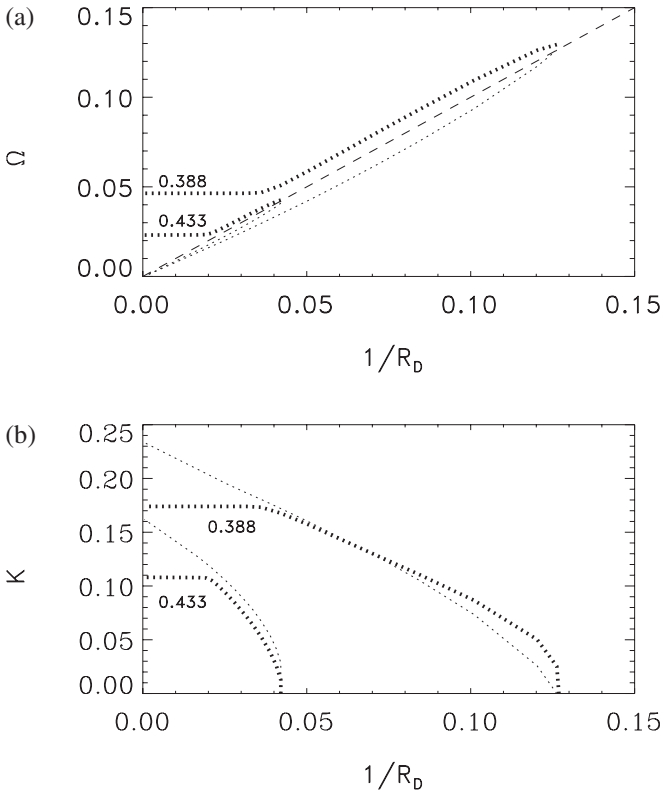

FIG. 3. Parameters of the rotating patterns vs the inverse disk radius, obtained as a solution of the free-boundary problem for two different values: the excitability $B=0.388$ and 0.433. (a) Angular velocity of a spot (thin dotted lines) and of a spiral wave (thick dotted lines). The relationship (16) with $K_{DR}=0$ is shown by a dashed line. (b) The curvature of the spot front K_{DR} near the disk boundary (thin dotted lines) and the front curvature K_Q at the point Q of the spiral front (thick dotted lines).

Hence, due to Eq. (16), both angular velocities approach $\Omega=1/R_D$ at the critical point, as can be seen in Fig. 2.

The relationship between the angular velocity Ω and the radius of a disk is illustrated in Fig. 3(a). For a rotating spot this relationship looks rather trivial. Since we are dealing with a weakly excitable medium, the curvature of the spot front near the disk boundary remains rather small. Relation (16) predicts in this case a linear increase of the angular velocity. Approximately such a linear increase can be seen in Fig. 3(a).

The similar dependence for a spiral wave is more complicated and includes three characteristic regions. Until the disk radius is sufficiently large the angular velocity of a spiral wave and the curvature K_Q are not influenced by the disk size. Due to Eq. (16), within this range of R_D the curvature K_{DR} can be approximated as $K_{DR}=-\Omega_0 R_D$, where Ω_0 is the angular velocity in the limit $R_D\to\infty$. Within the next range of R_D the curvature K_{DR} remains negative, but its absolute value becomes rather small. The angular velocity is approximately proportional to $1/R_D$ here, and the curvature K_Q decreases with $1/R_D$. Near some critical value of R_D the monotonous increase of Ω abruptly stops. At the spiral-spot bifurcation point both curvatures K_{DR} and K_Q vanish and the angular velocity of a spiral wave coincides with the angular

velocity of a spot. Expression (16) with $K_{DR}=0$ should be valid at all bifurcation points independently of the parameter B. This statement is verified in Fig. 3(a), where the relation (16) is depicted by a dashed line.

Note that the monotonous increase of the angular velocity of a spiral with the inverse disk size has been explained earlier in the framework of a kinematical theory [13]. However, this theory has been based on the wrong assumption that the curvature K_Q at the point Q is a characteristic of the medium and does not depend on the disk radius. Figure 3(b) shows that K_Q depends on the disk size and vanishes at the spiral-spot bifurcation point. Thus the free-boundary approach explains why a stationary rotating spiral wave can be observed only in a disk of a sufficiently large size. The existence of such a restriction has been experimentally observed earlier [16].

IV. SPIRAL WAVES IN AN UNBOUNDED MEDIUM

It is well-known that the influence of the disk boundary on a rotating spiral wave decreases very rapidly with the disk radius [13,14]. In the majority of the experimental studies the medium size is rather large and spiral waves are moving as unbounded spirals. Therefore a generalization of the previous analysis to the case of an infinitely large disk size is very important.

The corresponding consideration is rather similar to the one used for a spiral within a disk of a finite size. First, one should determine the outer part of the front and its angular velocity Ω for a given value K_Q. The selected solution has to satisfy the boundary conditions (20) and the condition (21) should be change to

$$C_n^+(\infty) = 1. \tag{23}$$

The next step is to determine the inner part of the front, in particular the velocity C_t of the phase change point. After this, starting with the conditions (18) and using a trial and error method, one must find out the value of B corresponding to the solution satisfying the boundary condition

$$C_n^-(-\infty) = 1. \tag{24}$$

Repetition of this process for different K_Q yields the dependence $B=B_S(K_Q)$. Since the angular velocity Ω is also a function of K_Q, we get the relationship $\Omega=\Omega_S(B)$, which is shown in Fig. 2. This monotonically decreasing function vanishes at $B=B_c\approx 0.535$ and a spiral wave degenerates here into a critical finger. The dependencies $\Omega=\Omega_{RS}(B,R_D)$, obtained for spirals rotating within two disks of different radii, approach this relationship, when B is small enough or R_D becomes larger.

As well as in the case of a disk, the curvature K_Q is an important intermediate parameter of the free-boundary problem. The selected values of K_Q are shown in Fig. 4(a). It turns out that within the range $0<B_c-B<0.25$ the curvature K_Q can be approximated with an accuracy of 5% as

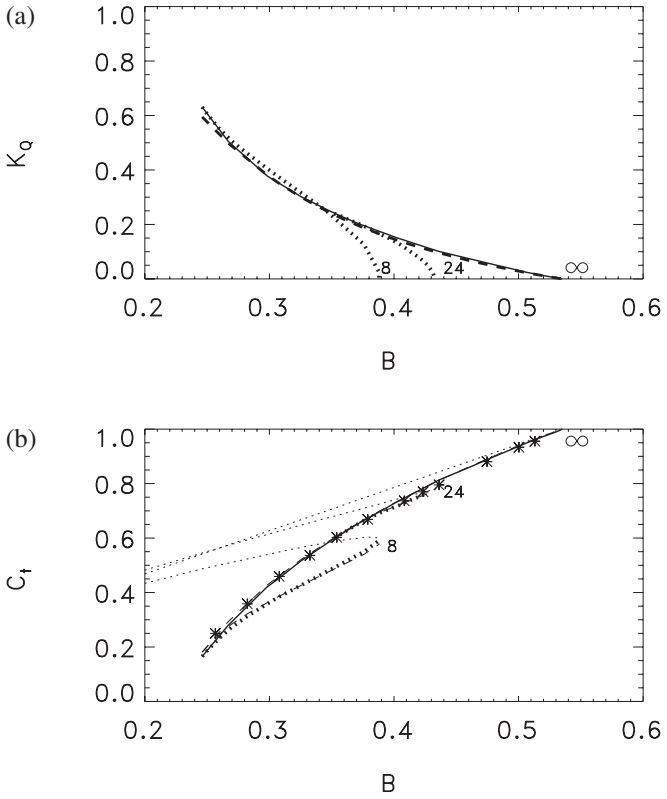

FIG. 4. Front curvature K_Q (a) and the tangential velocity C_t (b) obtained as a solution of the free-boundary problem for an unbounded spiral (thick solid). Corresponding values obtained for two different disk radii R_D are shown by thick dotted lines. Thin dotted lines depict the velocity C_t computed for spots circulating along the no-flux boundary of the disks. The predictions following from Eqs. (25) and (28) are shown by dashed lines. Separate stars depict results of direct integrations of the models (1) and (2).

$$K_Q = 0.691\,\delta B + 0.6(\delta B)^{3/2} + 8.5(\delta B)^3 + 48.0(\delta B)^5, \tag{25}$$

where $\delta B=B_c-B$. The linear term of this strongly nonlinear relationship coincides with an asymptotic derived in [9] for $\delta B \ll 1$ and provides an accuracy of about 10% only within a narrow region $\delta B<0.02$.

An analytical expression for the angular velocity of an unbounded spiral as a function of K_Q has been derived earlier [4],

$$\Omega = 0.685K_Q^{3/2} - 0.06K_Q^2 - 0.293K_Q^3. \tag{26}$$

Therefore Eqs. (25) and (26) provide an analytical prediction for the angular velocity of an unbounded spiral, which is shown by a dashed line in Fig. 2.

The tip velocity C_t is another intermediate parameter of the free-boundary problem. The selected values of C_t are shown in Fig. 4(b). The data obtained for an unbounded spiral determine a unique relationship between C_t and the selected value of the angular velocity Ω, which can be approximated as

$$\Omega = 0.198(1 - C_t)^{3/2} + 0.133(1 - C_t)^2. \quad (27)$$

The first term in this approximation coincides with an asymptotic derived in [9], which is valid for $C_t \approx 1$. The approximation (27) provides a nice accuracy within the whole range $0 < C_t < 1$.

It is important to stress that in the case of a stabilized wave segment the tip velocity is a linear function of the parameter B [6], shown by a thin dotted straight line in Fig. 4(b). One can see that the tip velocity is close to this asymptotic for $B \approx B_c$, but strongly deviates from this linear relationship, when B becomes smaller. It was found out that the observed relationship can be expressed with a high accuracy as

$$C_t = 1 - (B_c - B)/0.63 - 1.47\Omega. \quad (28)$$

This approximation is valid not only for an unbounded spiral, but as well for spiral waves within a disk. Since a stabilized wave segment undergoes a translational motion with $\Omega = 0$, this expression can be used in this case, too.

To obtain an explicit expression specifying the tip velocity C_t of an unbounded spiral for a given parameter B, Eq. (27) can be substituted into Eq. (28) that gives

$$C_d - 0.291C_d^{3/2} - 0.195C_d^2 = (B_c - B)/0.63, \quad (29)$$

where $C_d = 1 - C_t$.

Thus the angular velocity Ω of an unbounded spiral, tangential velocity of its tip C_t and the curvature K_Q at the point Q of its front are uniquely determined by the parameter B, which characterizes the medium excitability. Note that this value can be expressed through the measurable characteristics of the wave patterns, namely, the propagation velocity of a planar wave, c_0, and the duration of the activator pulse, d_u. To this aim, Eq. (10) should be considered in a region far away from the rotation center, where the front curvature is negligibly small and $c_n^- = -c_0$. Then the time interval between the front and the back of the activator pulse reads

$$d_u = \frac{\gamma^+(r) - \gamma^-(r)}{\omega} = \frac{2\Delta}{G^* \epsilon}. \quad (30)$$

Substitution of this expression into Eq. (15) yields

$$B = \frac{2D}{c_0^2 d_u}. \quad (31)$$

To obtain this expression, only the structure of the model (1) is used independently on the details of the nonlinear kinetics specified by Eq. (2). That gives an opportunity to extrapolate the results of the above study to other types of excitable kinetics.

To verify the theoretical predictions obtained from the solution of the free-boundary problem, we performed direct integrations of Eqs. (1) and (2) with $D = 1$. To reduce the medium refractoriness we took $\epsilon = \bar{\epsilon}$, then $G(u,v) > 0$, and $\epsilon = k_\epsilon \bar{\epsilon}$, then $G(u,v) < 0$, assuming $k_\epsilon \gg 1$ [22]. After this modification the refractory period of the medium becomes negligibly small with respect to the rotation period of an unbounded spiral. Namely this situation was assumed throughout the free-boundary consideration performed above. The explicit Euler integration method is used with discrete steps in time $\Delta t = 0.02$ and in space $\Delta x = 0.3$. In all computations a spiral wave is created by a special choice of the initial conditions on a mesh consisting of 500×500 nodes (for details see [8]). This mesh size is so large that the influence of the boundary can be neglected, and the resulting rotating patterns can be treated as unbounded spiral waves. The computational mesh is comoving with the spiral wave core in such a way that the spiral wave tip was always located at the mesh center. It allow us to compute spiral waves with extremely large core size.

Varying $\bar{\epsilon}$ in the range $0.001 < \bar{\epsilon} < 0.002$ and taking $k_\epsilon = 400$, the values of the angular velocity of unbounded spirals are computed and shown in Fig. 2 by separate stars. The computed values of the tip velocity are depicted in Fig. 4(b). It can be seen that the numerical data obtained are in a good quantitative agreement with the theoretical predictions. These values uniquely determine all essential characteristics of the spiral wave shape. For instance, the radius of the spital tip trajectory, $R_q = C_t/\Omega$, and the spiral wave pitch, $\lambda = 2\pi/\Omega$, are also predicted with a high accuracy. Small deviations of the numerical data from the theoretical predictions are due to some approximations that are used, e.g., a vanishing thickness of the interface between the resting and excited states and the linear relations (3) and (7) for the propagation velocity.

V. CONCLUSION

The free-boundary approach applied for patterns rotating in excitable media reveals the main selection mechanism based on an interaction between the front and the back of a rotating wave pattern. The discovered selection mechanism is not based on a dispersion relation for a wave train, as it was assumed in [12]. The dispersion relation was neglected in the presented consideration, but unique values of the rotation velocity and the spiral shape are still selected for a given medium excitability. The existence of a similar kind of a selection mechanism has been demonstrated numerically in Ref. [19]. A corresponding analytical consideration has been performed for the case of a critical finger in Ref. [7], where the crucial role of the parameter B was demonstrated. Later this consideration has been generalized to describe the case of an unbounded spiral wave [9].

However, our computations demonstrate that the asymptotic found in [9] is valid only in a close vicinity of the critical value B_c of the medium excitability and this asymptotic cannot be applied to study wave patterns rotating within a disk of a finite size.

In this paper the solution of the free-boundary problem has been solved numerically for the first time for wave patterns rigidly rotating within a disk of an arbitrary radius. The existence of an unknown wave pattern has been demonstrated, that is a spot rotating along the boundary of a disk. We have found that spots and spiral waves rotating within a disk represent coexisting solutions bifurcating from a critical point. Rotating spots are unstable, but can be stabilized by the application of a feedback to the medium excitability, in analogy to the stabilization of the wave segments [5,6].

We have shown that the curvature of the spiral front at the point Q is an intermediate parameter of the free-boundary problem, rather than an independent characteristic of the medium, as it was assumed earlier [4,13]. In particular, for rotating spiral waves K_Q depends on the disk radius and vanishes at the spiral-spot bifurcation point, as can be seen in Fig. 4(b).

We note that the solutions of the free-boundary problem obtained in a dimensionless form are universal. They can easily be applied to any weakly excitable media, as for this aim only the general characteristics of a two-component model should be known. The solutions computed numerically in a broad range of the medium parameters are also very important for the development of any kind of analytical predictions. For instance, they are in perfect agreement with the limiting case of the critical finger [7], with the description of the translating motion of the wave segments [6] and with asymptotic analysis of the unbounded spirals [9]. Analysis of the solutions obtained gives the opportunity to evaluate the accuracy of the proposed asymptotics.

The developed approach can be generalized to consider the role of the medium refractoriness, like it was done in [4,9,12,19], but that goes beyond the aim of this paper.

ACKNOWLEDGMENTS

This work was supported by the Deutsche Forschungsgemeinschaft (Grant No. SFB 555) and the National Science Foundation (Grant No. PHY05–51164). The author is thankful to H. Engel, V. Hakim, and A. Karma for helpful discussions.

[1] A. T. Winfree, *The Geometry of Biological Time* (Springer, Berlin, 2000).
[2] *Wave and Patterns in Biological and Chemical Excitable Media*, edited by V. Krinsky and H. Swinney (North-Holland, Amsterdam, 1991).
[3] *Chemical Waves and Patterns*, edited by R. Kapral and K. Showalter (Kluwer, Dordrecht, 1995).
[4] V. S. Zykov, *Simulation of Wave Processes in Excitable Media* (Manchester University Press, Manchester, 1987).
[5] E. Mihaliuk, T. Sakurai, F. Chirila, and K. Showalter, Phys. Rev. E **65**, 065602(R) (2002).
[6] V. S. Zykov and K. Showalter, Phys. Rev. Lett. **94**, 068302 (2005).
[7] A. Karma, Phys. Rev. Lett. **66**, 2274 (1991).
[8] A. S. Mikhailov and V. S. Zykov, Physica D **52**, 379 (1991).
[9] V. Hakim and A. Karma, Phys. Rev. E **60**, 5073 (1999).
[10] D. Margerit and D. Barkley, Chaos **12**, 636 (2002).
[11] A. M. Pertsov, E. A. Ermakova, and A. V. Panfilov, Physica D **14**, 117 (1984).
[12] J. J. Tyson and J. P. Keener, Physica D **32**, 327 (1988).
[13] V. A. Davydov and V. S. Zykov, JETP **76**, 414 (1993).
[14] I. Aranson, D. Kessler, and I. Mitkov, Physica D **85**, 142 (1995).
[15] V. S. Zykov and S. C. Müller, Physica D **97**, 322 (1966).
[16] N. Hartmann, M. Bär, I. G. Kevrekidis, K. Krischer, and R. Imbihl, Phys. Rev. Lett. **76**, 1384 (1996).
[17] P. C. Fife, J. Stat. Phys. **39**, 687 (1985).
[18] A. Bernoff, Physica D **53**, 125 (1991).
[19] P. Pelce and J. Sun, Physica D **48**, 353 (1991).
[20] D. Kessler and R. Kupferman, Physica D **97**, 509 (1996).
[21] F. B. Gul'ko and A. A. Petrov, Biofizika **17**, 261 (1972).
[22] V. S. Zykov, Biophysics (Engl. Transl.) **31**, 940 (1986).